Proceedings of the ASME 2010 International Design Engineering Technical Conferences & Computers and Information in Engineering Conference
IDETC/CIE 2010
August 15 - August 18, 2010, Montreal, Qeubec, Canada

DETC2010- 28953

NONLINEAR CONSTRAINT MODEL FOR SYMMETRIC THREE-DIMENSIONAL BEAMS

Shiladitya Sen* and Shorya Awtar
Precision Systems Design Laboratory
Mechanical Engineering, University of Michigan
Ann Arbor MI 48109

ABSTRACT

The constraint-based design of flexure mechanisms requires a qualitative and quantitative understanding of the constraint characteristics of flexure elements that serve as constraints. This paper presents the constraint characterization of a slender, uniform and symmetric cross-section, spatial beam, which is one of the most basic flexure elements used in three-dimensional flexure mechanisms. The constraint characteristics of interest, namely stiffness and error motions, are determined from the non-linear load-displacement relations of the beam. Appropriate simplifying assumptions are made in deriving these relations so that relevant non-linear effects (load-stiffening, kinematic, and elastokinematic) are captured in a compact, closed-form, and parametric manner. The resulting spatial beam constraint model is shown to be accurate, using non-linear finite element analysis, within a load and displacement range of practical interest. The utility of this model lies in the physical and analytical insight that it offers into the constraint behavior of a spatial beam flexure, its use in 3D flexure mechanism geometries, and fundamental performance tradeoffs in flexure mechanism design.

1. INTRODUCTION AND BACKGROUND

Flexure mechanisms are elastically deformable structures that are commonly used in machines and instruments to provide motion guidance and load bearing [1-3]. One of the many approaches employed in the synthesis of flexure mechanisms is constraint-based design [4]. In this approach, flexure mechanism synthesis is addressed as an exercise in creating the appropriate geometric arrangement of rigid bodies interconnected by constraints to satisfy certain desired mobility requirements on the rigid bodies. One of the strengths of constraint-based design is that it is conducive not only to planar (2D) geometries but also to spatial (3D) ones. However, while this approach is effective in generating conceptual designs, a more comprehensive assessment of performance and tradeoffs in the resulting flexure mechanism requires a qualitative and quantitative understanding of the constraint characteristics of the flexure elements that serve as constraints in the design.

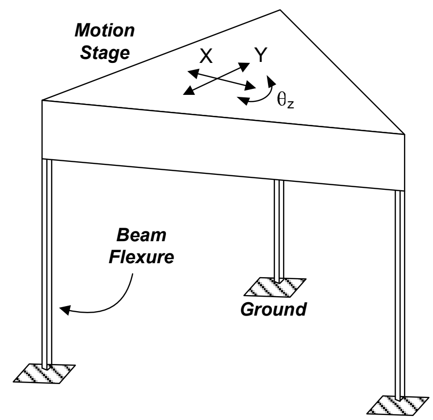

Fig.1 A 3-DoF Spatial Flexure Mechanism

It has been previously established that while flexure elements are highly desirable as constraints given of their lack of friction and backlash, their reliance on elastic deformation to produce motion results in several deviations from ideal constraint behavior [5, 6]. This is highlighted qualitatively via the example of Fig.1, which illustrates a simple 3-D flexure mechanism comprising a rigid Motion Stage supported by three beam flexures.

It is evident that that the three beam flexures are arranged such that the out-of-plane motions of the Motion Stage are constrained, while in-plane motions are allowed. Since the nominal stiffness in the three in-plane directions (X, Y, Θ_Z) is much lower than that of the three out-of-plane directions (Θ_X, Θ_Y, Z), it is rational to recognize the former as Degrees of Freedom (DoF) and the latter as Degrees of Constraint (DoC). While ideally, one would expect zero stiffness and infinite motion range in the DoF directions, and infinite stiffness and

*Corresponding Author (shiladit@umich.edu, 734-615-3595)

zero motions in the DoC directions, that is clearly not the case here. Given the inherent nature of flexure beams, the following observations may be made about the performance of this flexure mechanism:

1. The in-plane motions (DoF) of the stage lead to undesired error motions in the out-of-plane (DoC) directions due to the arc-length conservation of each beam flexure.
2. The out-of-plane load bearing capacity (DoC stiffness) reduces with increasing in-plane motions (DoF).
3. The presence of large out-of-plane loads (DoC) alters the in-plane (DoF) stiffness and therefore range of motion.

In order to quantify the above performance metrics (motion range, load bearing capacity, stiffness, and error motions) and associated tradeoffs, it is essential to have a mathematical model of the constraint behavior of the individual beams employed in this mechanism. Additionally, this model should be closed-form and parametric to enable design optimization, and simple enough to be used in more complex flexure mechanism geometries where performance limitations and tradeoffs may not be physically obvious as above.

While a linear elastic load-displacement model is simple, closed-form and parametric, it fails to capture the above observations, all of which are consequences of certain non-linearities in spatial beam mechanics. Several sources of non-linearities in spatial beam mechanics have been modeled and studied in the literature. These include beam arc length conservation [5], beam curvature [5, 7], the application of load-equilibrium in the deformed beam configuration [5, 8, 9], and out-of-plane and in-plane distortion of plane cross-sections [8]. For long and slender beams with a uniform cross-section, it may be rationalized that plane sections remain plane [10, 11], normal to the neutral axis, and undistorted within plane even after deformation. However, the remaining three sources of non-linearities may not be ignored for displacements of the order of the beam length. However, retaining all these non-linearities leads to a mathematically complicated formulation that can be only be solved by numerical methods such as Finite Element Analysis (FEA). While FEA is highly versatile, powerful, and accurate, its main limitation from a design stand-point is the lack of closed-form parametric results.

Since most flexure mechanisms operate within a DoF motion range such that the constituent beam deformation is less than 10% of the beam length, the inclusion of all the above non-linearities is not necessary. It may be shown that the beam curvature non-linearity is of limited consequence in this motion range [5, 6, 8]. However, non-linearities associated with arc-length conservation and application of load equilibrium in deformed configuration certainly play an important role in stiffness and error motions for displacements as small as the beam thickness and therefore have to be included. Therefore, for this 'intermediate' displacement range, relevant to flexure mechanism design, the desired goal is to capture only these pertinent non-linearities in spatial beam mechanics and ignore the rest to allow for a compact, closed-form, and parametric model.

This objective has been accomplished in the past for planar (2D) beams via the Beam Constraint Model (BCM) [5]. The BCM accurately captures the constraint characteristics of a planar beam flexure with generalized end-loads, initial and boundary conditions, and beam shape. However, such characterization does not exist for spatial beams as yet, which provides the motivation for this paper.

Although spatial beam mechanics has been modeled extensively in the past literature [8, 10, 11], we start from the first principles, for the sake of clarity and completeness, in Section 2 to analytically define the beam deformation. A transformation that relates undeformed and deformed configurations of the beam via Euler angles is stated. Differentiation of this transformation matrix along the deformed beam's neutral axis leads to the quantification of beam curvature in the two bending planes. This beam deformation is employed to derive a non-linear strain formulation. All approximations made throughout this process to retain or drop any given source of non-linearity are highlighted.

In Section 3, the strain expression and stress-strain constitutive relations are used to apply load equilibrium at an arbitrary cross-section along the deformed beam's neutral axis, which leads to three governing equations of the spatial beam – two for bending and one for twisting.

To analytically solve these beam governing equations simultaneously, a sub-class of uniform cross-section spatial beams defined by ($I_{yy}=I_{zz}$ and $I_{yz}=0$)[†] and referred to as symmetric cross-section beams, is considered this point onwards. This assumption tends to simplify the beam governing differential equations, without a significant loss in the utility of the final results. These equations are solved in Section 4 to derive relations between the six end-loads and six end-displacements of the beam. Transcendental expressions in these relations are expanded and truncated to retain the most significant terms and yield a compact closed-form beam model. The design insights allowed by this model in terms of constraint characteristics of the spatial beam are discussed. This closed-form spatial BCM is verified via non-linear FEA in Section 5, and is shown to be within 5% agreement. Concluding remarks and plans for future work are presented in Section 6.

2. SPATIAL BEAM DEFORMATION AND NON-LINEAR STRAIN FORMULATION

Fig.2 illustrates an initially-straight uniform cross-section beam fixed to ground at one end, and subjected to three forces $\boldsymbol{F_{XL}}$, $\boldsymbol{F_{YL}}$ and $\boldsymbol{F_{ZL}}$ and three moments $\boldsymbol{M_{XL}}$, $\boldsymbol{M_{YL}}$ and $\boldsymbol{M_{ZL}}$ acting at its free end. U_{XL}, U_{YL} and U_{ZL} represent the displacements of the beam's free end in its deformed configuration. These loads and displacements are expressed in the fixed XYZ coordinate frame. The beam geometry is specified by its length L, which is assumed to be much larger than its thickness, T_Y and T_Z in the Y

[†] See Section 2 for coordinate axis nomenclature

and Z directions respectively. In terms of constraint behavior, it is qualitatively evident that this spatial beam flexure imposes one DoC along the X axis (axial direction), and allows five DoF – translations and rotations along the Y and Z axes (transverse directions), and rotation along the X axis (twisting direction).

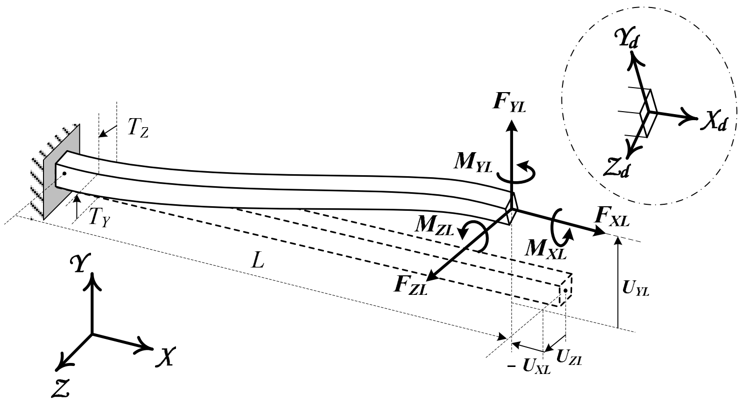

Fig.2 Spatial Beam Flexure: Undeformed and Deformed

For a long slender beam subjected to pure bending and torsion, symmetry arguments justify the Bernoulli assumption that plane sections prior to deformation will remain plane and perpendicular to the neutral axis after deformation [12]. Even though these symmetry arguments do not apply to cross-sections close to the beam ends, or in the presence of transverse forces, previous studies [12] confirm that the Bernoulli assumption is closely maintained as long as transverse displacements are within 10% of the beam length.

A direct consequence of the Bernoulli assumption is that shear strain components parallel to the beam axis (γ_{xy} and γ_{zx}) are close to zero. Consequently, stress-strain constitutive relations imply that the corresponding shear stress components ($\boldsymbol{\tau}_{yx}$ and $\boldsymbol{\tau}_{zx}$) are also small. Further, since the beam side walls are free of any loading and since the beam thickness along the Y and Z directions is much smaller compared to its length, it may be argued that that stress components $\boldsymbol{\sigma}_{yy}$ and $\boldsymbol{\sigma}_{zz}$ also remain close to zero over the beam cross-section. Next, we recall the Y direction elemental load equilibrium condition expressed in terms of stresses:

$$\frac{\partial \boldsymbol{\tau}_{yx}}{\partial x}+\frac{\partial \boldsymbol{\sigma}_{yy}}{\partial y}+\frac{\partial \boldsymbol{\tau}_{yz}}{\partial z}=0$$

Since $\boldsymbol{\sigma}_{yy}$ and $\boldsymbol{\tau}_{yx}$ ≈ 0, the above equation implies that $\partial \boldsymbol{\tau}_{yz}/\partial z \approx 0$. A similar argument made with the Z direction stresses leads to $\partial \boldsymbol{\tau}_{zy}/\partial y \approx 0$. This implies that the variation of $\boldsymbol{\tau}_{yz}$ along the Y or Z axis of the cross-section is insignificant, which in turn implies that the corresponding shear strain γ_{yz} remains constant within the cross-section plane. Now since γ_{yz} is zero at the cross-section's centroid, through which the neutral axis passes, γ_{yz} should remain close to zero throughout the cross-section. The final conclusion drawn here is that the in-plane distortion of a plane cross-section, after deformation, can also be ignored for a long slender beam[1].

Next, to define the deformed configuration of the beam, a second coordinate frame $X_dY_dZ_d$ is introduced. While shown only at the beam end in Fig.2, such a deformed frame may be constructed for any given axial cross-section location of the deformed beam. The X_d axis is tangent to the deformed neutral axis at the axial location of interest. The Y_d and Z_d axes define the un-distorted cross-sectional plane normal to the neutral axis of the deformed beam, and correspond to the Y and Z axes, respectively, of the same cross-sectional plane in the undeformed beam.

$$\begin{Bmatrix}\hat{i}_d\\ \hat{j}_d\\ \hat{k}_d\end{Bmatrix}=\left[T\right]\begin{Bmatrix}\hat{i}\\ \hat{j}\\ \hat{k}\end{Bmatrix} \tag{1}$$

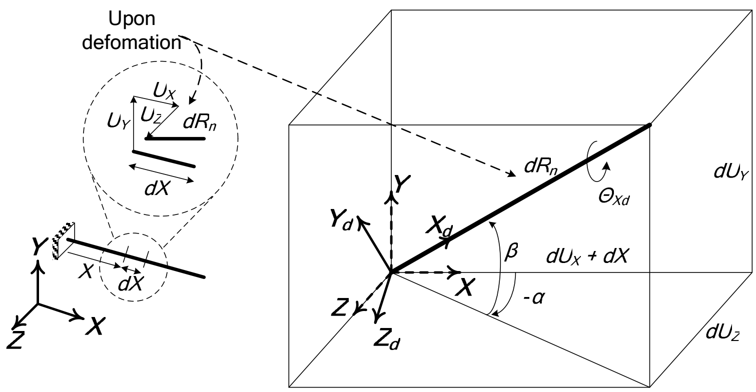

Fig.3: Axial Element of a Spatial Beam: Undeformed and Deformed

To obtain a suitable expression for the axial strain, it is important to be able to relate the deformed configuration of the beam to its undeformed configuration. Also since load equilibrium shall be considered in the deformed beam configuration while end loads are expressed in the undeformed coordinates, a coordinate transformation between the two above-defined frames is necessary. Therefore, we introduce a coordinate transformation matrix $[T]$ that relates the unit vectors $\hat{i}_d$, $\hat{j}_d$ and $\hat{k}_d$ along the deformed coordinate frame $X_dY_dZ_d$ to the unit vectors $\hat{i}$, $\hat{j}$ and $\hat{k}$ along the undeformed coordinate frame XYZ. Since we would like to state the final load-displacement results for the spatial beam in the undeformed coordinate frame, it is essential that matrix $[T]$ is expressed in term of variables defined in the undeformed coordinate frame XYZ.

In Fig. 3. U_X, U_Y, and U_Z – all functions of X – represent the displacements along the XYZ frame, of a certain point on the neutral axis of the deformed beam that was located at (X, 0,

[1] Since there are small but finite strains ε_{yy} and ε_{zz} resulting from $\boldsymbol{\sigma}_{xx}$ due to the Poisson effect, there is indeed some in-plane distortion of the cross-section. In thicker beams, this distortion is non-negligible and leads the *anti-clastic* beam curvature [12].

0) on the beam before deformation. To determine [T], let us consider a differential beam element, originally at this location, in its undeformed (dX) and deformed (dR_n) configurations. The subscript 'n' in dR_n denotes the neutral axis.

The transformation matrix may then be expressed in terms of the three Euler angles -α, β and θ_{xd} shown in Fig. 3. α is a CW rotation about the original Y axis; β is a CCW rotation about an intermediate Z axis created after the first rotation; and θ_{xd} is a CCW rotation about the final X_d axis. Using sine and cosine relations, angles α and β are substituted by dU_X, dU_Y, dU_Z, and dR_n, to yield the following expression for [T]:

$$\begin{bmatrix} \Delta_{YZ} & U_Y^+ & U_Z^+ \\ -\frac{c(\Theta_{xd})U_Y^+\Delta_{YZ}}{\Delta_Y}-\frac{s(\Theta_{xd})U_Z^+}{\Delta_Y} & c(\Theta_{xd})\Delta_Y & -\frac{c(\Theta_{xd})U_Y^+U_Z^+}{\Delta_Y}+\frac{s(\Theta_{xd})\Delta_{YZ}}{\Delta_Y} \\ \frac{s(\Theta_{xd})U_Y^+\Delta_{YZ}}{\Delta_Y}-\frac{c(\Theta_{xd})U_Z^+}{\Delta_Y} & -s(\Theta_{xd})\Delta_Y & \frac{s(\Theta_{xd})U_Y^+U_Z^+}{\Delta_Y}+\frac{c(\Theta_{xd})\Delta_{YZ}}{\Delta_Y} \end{bmatrix}$$

where, the superscript $^+$ refers to derivative with respect to R_n,

$$\Delta_{YZ} \triangleq \sqrt{1-\left(\frac{dU_Y}{dR_n}\right)^2-\left(\frac{dU_Z}{dR_n}\right)^2} \;,\; \Delta_Y \triangleq \sqrt{1-\left(\frac{dU_Y}{dR_n}\right)^2} \;,$$

and $dR_n = \sqrt{(dX + dU_X)^2 + dU_Y{}^2 + dU_Z{}^2}$

$$c(\Theta_{xd}) \triangleq \cos(\Theta_{xd}) \quad ; \quad s(\Theta_{xd}) \triangleq \sin(\Theta_{xd}) \tag{2}$$

Recalling that the transformation matrix [T] varies with the location along the neutral axis, its rate of change with R_n gives another useful relation. The derivative of [T] with respect to R_n may be expressed in the following form:

$$\frac{d[T]}{dR_n} = \begin{bmatrix} 0 & \kappa_{zd} & -\kappa_{yd} \\ -\kappa_{zd} & 0 & \kappa_{xd} \\ \kappa_{yd} & -\kappa_{xd} & 0 \end{bmatrix}[T] = [\kappa][T] \tag{3}$$

where,

$$\kappa_{Xd} = \frac{\Theta_{xd}^+\Delta_{YZ}\Delta_Y - U_Z^{++}U_Y^+\Delta_Y - U_Y^{++}U_Z^+\left(U_Y^+\right)^2}{\Delta_{YZ}\Delta_Y{}^2}$$

$$\kappa_{Yd} = \frac{\sin(\Theta_{xd})U_Y^{++}\Delta_{YZ} - \cos(\Theta_{xd})U_Z^{++} - \cos(\Theta_{xd})U_Y^+U_Z^+U_Y^{++}}{\Delta_{YZ}\Delta_Y{}^2} + \frac{\cos(\Theta_{xd})U_Z^{++}\left(U_Y^+\right)^2}{\Delta_{YZ}\Delta_Y{}^2}$$

$$\kappa_{Zd} = \frac{\cos(\Theta_{xd})U_Y^{++}\Delta_{YZ} + \sin(\Theta_{xd})U_Z^{++} + \sin(\Theta_{xd})U_Y^+U_Z^+U_Y^{++}}{\Delta_{YZ}\Delta_Y} - \frac{\sin(\Theta_{xd})U_Z^{++}\left(U_Y^+\right)^2}{\Delta_{YZ}\Delta_Y}$$

It may be noted that the skew-symmetric matrix [κ] is analogous to the angular velocity matrix [ω] associated with the rigid-body rotation transformation [13]. Upon further simplification in Section 3, it will become obvious that κ_{Yd} and κ_{Zd} are related to the beam curvature in the X_dY_d and X_dZ_d planes.

Next, we move on to determining an expression for the axial strain ε_{xx} [12]. As argued above, all other components of strain are small and of little consequence in a long slender beam.

$$\varepsilon_{XX} = \frac{|dR|-|dX|}{|dX|} \tag{4}$$

Here dX and dR represent an undeformed and deformed differential length fiber, parallel to the beam neutral axis but not necessarily on the neutral axis. This undeformed fiber dX is taken to be parallel to the undeformed neutral axis at a generic location (X, Y, Z), and becomes dR upon deformation. Thus, dR is slightly different from the dR_n shown in Fig.3.

The post-deformation location of a point, which was located at (X, Y, Z) w.r.t. XYZ frame before deformation, is simply obtained by considering the neutral axis displacements U_X, U_Y and U_Z and the Euler angle rotations of the relevant cross-sectional plane. Since in-plane and out-of-plane distortion of cross-sectional planes has been ignored, the Y_d and Z_d coordinates of a certain point on a cross-section plane after deformation will be the same as the Y and Z coordinates of this point before deformation. This knowledge, in conjunction with transformation matrix [T], helps express the post-deformation coordinates of the point of interest in the XYZ frame. Taking a differential of these coordinates helps provide the deformed length dR of an initially undeformed fiber dX. Substituting this value of dR in Eq.(4) yields:

$$\varepsilon_{XX} = \frac{dU_X}{dX} + \frac{1}{2}\left(\frac{dU_Y}{dX}\right)^2 + \frac{1}{2}\left(\frac{dU_Z}{dX}\right)^2 - Y\kappa_{Zd} + Z\kappa_{Yd} - YZ\kappa_{Zd}\kappa_{Yd} + \frac{1}{2}\kappa_{Xd}{}^2\left(Y^2+Z^2\right) + \frac{1}{2}Y^2\kappa_{Zd}{}^2 + \frac{1}{2}Z^2\kappa_{Yd}{}^2 \tag{5}$$

The above procedure is standard and a step-by-step detailed derivation may be found in previous work [8, 14]. At this stage, the slender beam geometry and small transverse displacements (~ $0.1L$), allow us to make some further simplifications. Over this displacement range, κ's, which approximately represent the beam curvature, are also be of the order of $0.1L$. Furthermore, U_Y' and U_Z' are of the order of 0.1 and U_X' is ~ 0.01. The coordinate variables Y and Z, describing the location on the cross-sectional plane, are less than or equal to T_Y and T_Z, both of which are at least one order smaller than L. Based on these observations, it may be seen that the last four terms in Eq.(5) are at least two orders smaller than the remaining terms, and are therefore dropped this point onwards.

3. SPATIAL BEAM GOVERNING EQUATIONS

The moments at any cross-section along the beam's neutral axis is obtained by integrating the force acting on a differential area of the cross-section multiplied by its perpendicular distance from the axis about which the moment is to be considered. The moments about the deformed co-ordinate axes Y_d and Z_d are given below. Since stresses σ_{yy} and σ_{zz} are negligible, the axial stress σ_{xx} is simply obtained by multiplying the axial strain ε_{xx} by elastic modulus E. These integrations are carried out in the displaced configuration of each cross-section. However, since it is assumed that the cross-sections do not distort either in-plane or out-of-plane, the integrand can be considered simply in terms of *Y* and *Z* coordinates, with respect to the cross-section itself.

$$\begin{aligned}\boldsymbol{M_{ZD}} &= -\int_0^A YE\varepsilon_{XX}dA = E\int_0^A Y^2\kappa_{Zd}dA \\ &-E\int_0^A\left[\frac{dU_X}{dX}+\frac{1}{2}\left(\frac{dU_Y}{dX}\right)^2+\frac{1}{2}\left(\frac{dU_Z}{dX}\right)^2+Z\kappa_{Yd}\right]YdA \\ \boldsymbol{M_{YD}} &= \int_0^A ZE\varepsilon_{XX}dA = E\int_0^A Z^2\kappa_{Yd}dA \\ &+E\int_0^A\left[\frac{dU_X}{dX}+\frac{1}{2}\left(\frac{dU_Y}{dX}\right)^2+\frac{1}{2}\left(\frac{dU_Z}{dX}\right)^2-Y\kappa_{Zd}\right]ZdA\end{aligned} \tag{6}$$

By the definition of neutral axis and the symmetric beam cross-section assumption,

$$\int_0^A YdA = \int_0^A ZdA = \int_0^A YZdA = 0 \tag{7}$$

Furthermore since $\kappa_{X\mathrm{d}}$, κ_{Yd}, and κ_{Zd} are independent of the cross-sectional variables, they can be extracted out of the integrals in Eq.(6) to yield the following:.

$$\begin{aligned}&\boldsymbol{M_{YD}} = EI_{YY}\kappa_{Yd}, \qquad \boldsymbol{M_{ZD}} = EI_{ZZ}\kappa_{Zd} \\ &\text{where, } I_{YY} = \int_0^A Z^2dA \quad\text{and}\quad I_{ZZ} = \int_0^A Y^2dA\end{aligned} \tag{8}$$

It should be noted here that due to the assumption that plane sections do not distort and remain perpendicular to the neutral axis, the moments of area I_{yy} and I_{zz} are unaffected by the beam deformation. Furthermore, for a symmetric cross-section beam $I_{yy} = I_{zz} = I$.

Next, the twist in the beam, which occurs in the plane perpendicular to the deformed neutral axis, is dictated by the following governing equation [12]:

$$\begin{aligned}&\boldsymbol{M_{XD}} = GI_{XX}\kappa_{Xd} \\ &\text{where, } I_{XX} = \int_0^A\left(Y^2+Z^2\right)dA = 2I\end{aligned} \tag{9}$$

Eqs.(8) and (9) may be expressed in a matrix equation, true for any location along the beam's deformed arc-length:

$$\begin{Bmatrix}\kappa_{Xd}\\ \kappa_{Yd}\\ \kappa_{Zd}\end{Bmatrix} = \begin{bmatrix}\frac{1}{GI_{xx}} & 0 & 0\\ 0 & \frac{1}{EI_{yy}} & 0\\ 0 & 0 & \frac{1}{EI_{zz}}\end{bmatrix}\begin{Bmatrix}\boldsymbol{M_{XD}}\\ \boldsymbol{M_{YD}}\\ \boldsymbol{M_{ZD}}\end{Bmatrix} \tag{10}$$

This expression highlights the fact that small transverse deformations (~ *0.1L*), the beam governing equations (two bending and one twisting) are essentially decoupled in relating moments to curvatures in the $X_dY_dZ_d$ co-ordinate frame, at least to a second order approximation. However, since the deformed directions X_d, Y_d and Z_d continuously vary along the arc-length of the beam's deformed neutral axis, solving these equations is non-trivial. Instead, it is prudent to express the κ's and moments in the XYZ co-ordinate frame.

For small transverse displacements, U_Y and U_Z (~ *0.1L*), their derivatives, U_Y^+ and U_Z^+, are of the order *0.1L* while as U_X is of the order *0.01L*, its derivative U_X^+ is of the order of *0.01L*. This implies that the following approximations may be made with less than 1% error.

$$\frac{dU_X}{dR_n}\approx\frac{dU_X}{dX} \quad;\quad \frac{dU_Y}{dR_n}\approx\frac{dU_Y}{dX} \quad;\quad \frac{dU_Z}{dR_n}\approx\frac{dU_Z}{dX}$$

Using these approximations, matrices [*T*] and κ*'s* in Eq.(3) may be simplified as follows:

$$[T]\approx \tag{11}$$

$$\begin{bmatrix}1 & U_Y' & U_Z'\\ -\mathrm{c}(\Theta_{xd})U_Y'-\mathrm{s}(\Theta_{xd})U_Z' & \mathrm{c}(\Theta_{xd}) & -\mathrm{c}(\Theta_{xd})U_Y'U_Z'+\mathrm{s}(\Theta_{xd})\\ \mathrm{s}(\Theta_{xd})U_Y'-\mathrm{c}(\theta_{xd})U_Z' & -\mathrm{s}(\Theta_{xd}) & \mathrm{s}(\Theta_{xd})U_Y'U_Z'+\mathrm{c}(\Theta_{xd})\end{bmatrix}$$

$$\begin{aligned}\kappa_{Xd} &\approx \Theta_{Xd}'-U_Z''U_Y'\\ \kappa_{Yd} &\approx \sin(\Theta_{Xd})U_Y''-\cos(\Theta_{Xd})U_Z'\\ \kappa_{Zd} &\approx \cos(\Theta_{Xd})U_Y''+\sin(\Theta_{Xd})U_Z''\end{aligned} \tag{12}$$

The first equation in Eq.(12) shows that the total rate of change of twist angle Θ'_{Xd} is not only dependent on the twisting moment $\boldsymbol{M_{ZD}}$ (via κ_{Zd}), but also depends on transverse displacements. Being dependent on displacements alone rather than any loads, the $-U_Y'U_Z''$ is a result of a geometric constraint, and should ultimately contribute to a kinematic portion in the total twist angle.

Since U_Y'' and U_Z'' are the linearized curvature of the beam in the *XY* and *XZ* planes respectively, the latter two equations in Eq.(12) imply that, κ_{Xd} and κ_{Yd} are the literalized curvatures of the beam in X_dY_d and X_dZ_d planes, respectively, which agrees with the physical understanding of the deformed geometry.

The moments in the deformed configuration can be related to those in the undeformed orientation using the transformation matrix [*T*]. This transformation along with Eq.(12) may be used to simplify Eq.(10), to produce the following relation between displacements and moments, expressed in the XYZ frame.

$$\begin{Bmatrix}\kappa_{Xd}\\ U_Y''\\ U_Z''\end{Bmatrix} = \begin{bmatrix}\frac{1}{2GI} & \frac{U_Y'}{2GI} & \frac{U_Z'}{2GI}\\ -\frac{U_Z'}{EI} & 0 & \frac{1}{EI}\\ \frac{U_Y'}{EI} & -\frac{1}{EI} & \frac{U_Y'U_Z'}{EI}\end{bmatrix}\begin{Bmatrix}\boldsymbol{M_X}\\ \boldsymbol{M_Y}\\ \boldsymbol{M_Z}\end{Bmatrix}$$

$$\begin{aligned}&\Theta_{Xd}{}' = \frac{\boldsymbol{M_X}}{2GI}+\frac{U_Y'\boldsymbol{M_Y}}{2GI}+\frac{U_Z'\boldsymbol{M_Z}}{2GI}+U_Z''U_Y' && \text{(i)}\\ \Rightarrow\quad &U_Y'' = -\frac{U_Z'\boldsymbol{M_X}}{EI}+\frac{\boldsymbol{M_Z}}{EI} && \text{(ii)}\\ &U_Z'' = \frac{U_Y'\boldsymbol{M_X}}{EI}-\frac{\boldsymbol{M_Y}}{EI}+\frac{U_Y'U_Z'\boldsymbol{M_Z}}{EI} && \text{(iii)}\end{aligned} \tag{13}$$

Taking a closer look at the three equations we first observe that the second and third equation is independent of Θ_{Xd}, and therefore can be solve independent of the first equation. This independence from Θ_{Xd} occurs even without making the small angle approximations, $\cos(\Theta_{Xd}) \approx 1$ and $\sin(\Theta_{Xd}) \approx \Theta_{Xd}$, in the expression for $[T]$ given by Eq.(11). In fact, trigonometric identities all Θ_{Xd} terms simply drop out on their own. Secondly, we see that the second and third equations for bending in the Y and Z directions, respectively, are non-symmetrical. This is simply because in calculating the transformation matrix $[T]$ using Euler angles, the order in which the first two rotations are carried out breaks the symmetry between the Y and Z axes. In fact, if the first Euler angle rotation is carried out about the Z axis then Eq.(13)(ii) has the extra term instead of Eq.(13)(iii). But in any case, it can be shown that this nonlinear term in Eq.(13)(iii) is two orders of magnitude smaller than the remaining terms, for U_Y, $U_Z \sim 0.1L$ and $\Theta_{Xd} \sim 0.1$. Therefore, this term can be dropped, resulting in:

$$U''_Y = -\frac{U'_Z \boldsymbol{M_X}}{EI} + \frac{\boldsymbol{M_Z}}{EI} \qquad U''_Z = \frac{U'_Y \boldsymbol{M_X}}{EI} - \frac{\boldsymbol{M_Y}}{EI} \tag{14}$$

It is noted that all the variables in the above equation are in the undeformed coordinate frame even though the load equilibrium was carried out in the deformed frame. Taking a closer look at these equations, it may be recognized that $(-U_Z'\boldsymbol{M_X} + \boldsymbol{M_Z})$ and $(U_Y'\boldsymbol{M_X} - \boldsymbol{M_Y})$ are simply the effective bending moments, approximated to the second order, in the Z and Y directions, respectively.

It is noteworthy that with the approximations made so far, we have neither dropped all possible coupling and non-linear effects as in the case of a linear formulation; nor have we included every possible non-linearity such that a closed-form solution would be impossible. We have taken a middle path and have justified all approximations while doing so, to obtain a pair of symmetric, coupled bending equations independent of the twisting angle but dependent on the twisting moment. Additionally, we have a twisting equation with a strong dependence on bending moments as well as displacements.

4. END LOAD – DISPLACEMENT RELATIONS

$\boldsymbol{M_X}$, $\boldsymbol{M_Y}$ and $\boldsymbol{M_Z}$ at any X location may be determined by applying load equilibrium in the deformed beam configuration:

$$\begin{aligned} \boldsymbol{M_X}(X) &= \boldsymbol{M_{XL}} - \boldsymbol{F_{YL}}(U_{ZL} - U_Z) + \boldsymbol{F_{ZL}}(U_{YL} - U_Y) \\ \boldsymbol{M_Z}(X) &= \boldsymbol{M_{ZL}} + \boldsymbol{F_{YL}}(L - X) - \boldsymbol{F_{XL}}(U_{YL} - U_Y) \\ \boldsymbol{M_Y}(X) &= \boldsymbol{M_{YL}} - \boldsymbol{F_{ZL}}(L - X) + \boldsymbol{F_{XL}}(U_{ZL} - U_Z) \end{aligned} \tag{15}$$

The end loads $\boldsymbol{M_{ZL}}$, $\boldsymbol{M_{YL}}$, $\boldsymbol{F_{YL}}$, $\boldsymbol{F_{ZL}}$ and $\boldsymbol{F_{XL}}$ and the end displacements U_{ZL} and U_{YL} are shown in Fig.1. At this point in the analysis, we proceed to normalize all the loads and displacements per the following scheme:

$$\boldsymbol{m_{z1}} \triangleq \frac{\boldsymbol{M_{ZL}}L}{EI},\quad \boldsymbol{m_{y1}} \triangleq \frac{\boldsymbol{M_{YL}}L}{EI},\quad \boldsymbol{m_{x1}} \triangleq \frac{\boldsymbol{M_{XL}}L}{EI},\quad \boldsymbol{f_{z1}} \triangleq \frac{\boldsymbol{F_{ZL}}L^2}{EI},$$

$$\boldsymbol{f_{y1}} \triangleq \frac{\boldsymbol{F_{YL}}L^2}{EI},\quad \boldsymbol{f_{x1}} \triangleq \frac{\boldsymbol{F_{XL}}L^2}{EI},\quad u_y \triangleq \frac{U_Y}{L},\quad u_z \triangleq \frac{U_Z}{L},$$

$$u_{y1} \triangleq \frac{U_{YL}}{L},\quad u_{z1} \triangleq \frac{U_{ZL}}{L},\quad x \triangleq \frac{X}{L},\quad \theta_{xd} \triangleq \Theta_{Xd},\quad \theta_{xd1} \triangleq \Theta_{Xd1} \tag{16}$$

It should be noted here that from linear analysis for $\Theta_{Xd} \sim 0.1$, which is the range of twist considered in this paper, $\boldsymbol{m_{x1}}$ is also of the order of 0.1. Eq.(14) can now be rewritten using Eq.(15) and Eq.(16) as:

$$\begin{aligned} u''_y &= -u'_z \boldsymbol{m_{x1}} + \boldsymbol{f_{y1}}\left\{u'_z(u_{z1} - u_z)\right\} - \boldsymbol{f_{z1}}\left\{u'_z(u_{y1} - u_y)\right\} \\ &\quad + \boldsymbol{m_{z1}} + \boldsymbol{f_{y1}}(1 - x) - \boldsymbol{f_{x1}}(u_{y1} - u_y) \\ u''_z &= u'_y \boldsymbol{m_{x1}} + \boldsymbol{f_{y1}}\left\{u'_y(u_{z1} - u_z)\right\} - \boldsymbol{f_{z1}}\left\{u'_y(u_{y1} - u_y)\right\} \\ &\quad - \boldsymbol{m_{y1}} + \boldsymbol{f_{z1}}(1 - x) - \boldsymbol{f_{x1}}(u_{z1} - u_z) \end{aligned} \tag{17}$$

It can be easily observed that the non-linear terms in Eq.(17) are three orders smaller than the dominating bending moments since $\boldsymbol{m_{x1}}$, θ_{xd}, u_{y1}, u_{z1}, u_y, u_z, u'_y and u'_z are all of order 0.1 while $\boldsymbol{m_{y1}}$, $\boldsymbol{m_{z1}}$, $\boldsymbol{f_{x1}}$, $\boldsymbol{f_{y1}}$ and $\boldsymbol{f_{z1}}$ are all of the order 1. Dropping these terms results in the following simplification:

$$\begin{aligned} u''_y &= -u'_z \boldsymbol{m_{x1}} + \boldsymbol{m_{z1}} + \boldsymbol{f_{y1}}(1 - x) - \boldsymbol{f_{x1}}(u_{y1} - u_y) \\ u''_z &= u'_y \boldsymbol{m_{x1}} - \boldsymbol{m_{y1}} + \boldsymbol{f_{z1}}(1 - x) - \boldsymbol{f_{x1}}(u_{z1} - u_z) \end{aligned} \tag{18}$$

While other formulations for spatial beams include non-linear coupling of the bending direction equations [8, 10], our assumptions from the previous section lead to a pair of coupled but linear differential equations. This coupling arises from the twisting moment $\boldsymbol{m_{x1}}$, which contributes an additional load in both bending directions. In the absence of this twisting moment, the coupling vanishes, and bi-directional bending of the spatial beam becomes equivalent to the bending of two independent planar beams.

Upon double differentiation, Eq.(18) may be expressed as a first order ordinary differential matrix equation:

$$\begin{Bmatrix} u'''_y \\ u''_y \\ u'''_z \\ u''_z \end{Bmatrix}' = \begin{bmatrix} 0 & \boldsymbol{f_{x1}} & -\boldsymbol{m_{x1}} & 0 \\ 1 & 0 & 0 & 0 \\ \boldsymbol{m_{x1}} & 0 & 0 & \boldsymbol{f_{x1}} \\ 0 & 0 & 1 & 0 \end{bmatrix} \begin{Bmatrix} u'''_y \\ u''_y \\ u'''_z \\ u''_z \end{Bmatrix} \tag{19}$$

The four scalar equations represented above can be solved by first decoupling them. This may be done via the eigen-values and eigen-vectors of the square matrix in the above equation.

E-values: $\boldsymbol{\lambda_1} = \boldsymbol{\lambda}$, $\boldsymbol{\lambda_2} = -\boldsymbol{\lambda}$, $\boldsymbol{\lambda_3} = \dfrac{\boldsymbol{f_{x1}}}{\boldsymbol{\lambda}}$, $\boldsymbol{\lambda_4} = -\dfrac{\boldsymbol{f_{x1}}}{\boldsymbol{\lambda}}$

where, $\boldsymbol{\lambda} \triangleq \dfrac{1}{2}\sqrt{4\boldsymbol{f_{x1}} - 2\boldsymbol{m_{x1}}^2 + 2\boldsymbol{m_{x1}}\sqrt{\boldsymbol{m_{x1}}^2 - 4\boldsymbol{f_{x1}}}}$

E-vector matrix: $[Q] = \begin{bmatrix} -\boldsymbol{r} & -\boldsymbol{r} & -\dfrac{\boldsymbol{f_{x1}}}{\boldsymbol{r}} & -\dfrac{\boldsymbol{f_{x1}}}{\boldsymbol{r}} \\ -\dfrac{\boldsymbol{r}}{\boldsymbol{\lambda_1}} & -\dfrac{\boldsymbol{r}}{\boldsymbol{\lambda_2}} & -\dfrac{\boldsymbol{f_{x1}}}{\boldsymbol{\lambda_3 r}} & -\dfrac{\boldsymbol{f_{x1}}}{\boldsymbol{\lambda_4 r}} \\ \boldsymbol{\lambda_1} & \boldsymbol{\lambda_2} & \boldsymbol{\lambda_3} & \boldsymbol{\lambda_4} \\ 1 & 1 & 1 & 1 \end{bmatrix}$

where, $\boldsymbol{r} \triangleq \dfrac{1}{2}\left[\boldsymbol{m_{x1}} - \sqrt{\boldsymbol{m_{x1}}^2 - 4\boldsymbol{f_{x1}}}\right]$

The eigen-values λ_1, λ_2, λ_3 and λ_4 are distinct for non-zero $\boldsymbol{f}_{x1}$ values implying that the equations can be decoupled for $\boldsymbol{f}_{x1}$ non-zero [15][†]. The eigen-vectors are constitute the columns of the matrix $[Q]$. Using these eigen-values and eigen-vectors, the solution to Eq.(19) is simply given by:

$$\begin{Bmatrix} u_y''' \\ u_y'' \\ u_z''' \\ u_z'' \end{Bmatrix} = [Q] \begin{Bmatrix} c_1 e^{\lambda_1 x} \\ c_2 e^{\lambda_2 x} \\ c_3 e^{\lambda_3 x} \\ c_4 e^{\lambda_4 x} \end{Bmatrix} = \begin{bmatrix} -\boldsymbol{r} & -\boldsymbol{r} & -\frac{\boldsymbol{f}_{x1}}{\boldsymbol{r}} & -\frac{\boldsymbol{f}_{x1}}{\boldsymbol{r}} \\ -\frac{\boldsymbol{r}}{\lambda_1} & -\frac{\boldsymbol{r}}{\lambda_2} & -\frac{\boldsymbol{f}_{x1}}{\lambda_3 \boldsymbol{r}} & -\frac{\boldsymbol{f}_{x1}}{\lambda_4 \boldsymbol{r}} \\ \lambda_1 & \lambda_2 & \lambda_3 & \lambda_4 \\ 1 & 1 & 1 & 1 \end{bmatrix} \begin{Bmatrix} c_1 e^{\lambda_1 x} \\ c_2 e^{\lambda_2 x} \\ c_3 e^{\lambda_3 x} \\ c_4 e^{\lambda_4 x} \end{Bmatrix} \quad (20)$$

Here c_1, c_2, c_3 and c_4 are the constants of integration. From these four scalar equation, the general solution for the normalized transverse displacements u_y and u_z are given by:

$$\begin{aligned} u_y &= -\frac{\boldsymbol{r}}{\lambda_1^3} c_1 e^{\lambda_1 x} - \frac{\boldsymbol{r}}{\lambda_2^3} c_2 e^{\lambda_2 x} - \frac{\boldsymbol{f}_{x1}}{\lambda_3^3 \boldsymbol{r}} c_3 e^{\lambda_3 x} - \frac{\boldsymbol{f}_{x1}}{\lambda_4^3 \boldsymbol{r}} c_4 e^{\lambda_4 x} + c_5 x + c_6 \\ u_z &= \frac{c_1 e^{\lambda_1 x}}{\lambda_1^2} + \frac{c_2 e^{\lambda_2 x}}{\lambda_2^2} + \frac{c_3 e^{\lambda_3 x}}{\lambda_3^2} + \frac{c_4 e^{\lambda_4 x}}{\lambda_4^2} + c_7 x + c_8 \end{aligned} \quad (21)$$

The constants are solved in two steps. First the constants c_5, c_6, c_7 and c_8 are expressed in terms of c_1, c_2, c_3 and c_4 using the geometric boundary conditions arising from the spatial beam being rigidly fixed at one end:

$$u_y(0) = u_y'(0) = u_z(0) = u_z'(0) = 0 \quad \Rightarrow$$

$$\begin{Bmatrix} c_5 \\ c_6 \\ c_7 \\ c_8 \end{Bmatrix} = \begin{bmatrix} \frac{\boldsymbol{r}}{\lambda_1^2} & \frac{\boldsymbol{r}}{\lambda_2^2} & \frac{\boldsymbol{f}_{x1}}{\boldsymbol{r}\lambda_3^2} & \frac{\boldsymbol{f}_{x1}}{\boldsymbol{r}\lambda_4^2} \\ \frac{\boldsymbol{r}}{\lambda_1^3} & \frac{\boldsymbol{r}}{\lambda_2^3} & \frac{\boldsymbol{f}_{x1}}{\boldsymbol{r}\lambda_3^3} & \frac{\boldsymbol{f}_{x1}}{\boldsymbol{r}\lambda_4^3} \\ -\frac{1}{\lambda_1} & -\frac{1}{\lambda_2} & -\frac{1}{\lambda_3} & -\frac{1}{\lambda_4} \\ -\frac{1}{\lambda_1^2} & -\frac{1}{\lambda_2^2} & -\frac{1}{\lambda_3^2} & -\frac{1}{\lambda_4^2} \end{bmatrix} \begin{Bmatrix} c_1 \\ c_2 \\ c_3 \\ c_4 \end{Bmatrix} \quad (22)$$

The remaining four constants are solved using the free-end displacement boundary conditions:

$$u_y(1) = u_{y1}, \quad u_y'(1) = \theta_{z1}, \quad u_z(1) = u_{z1}, \quad u_z'(1) = -\theta_{y1} \quad \Rightarrow$$

$$\{c_1 \quad c_2 \quad c_3 \quad c_4\}^T = [C]\{u_{y1} \quad \theta_{z1} \quad u_{z1} \quad \theta_{y1}\}^T, \text{ where}$$

$$[C] \triangleq \begin{bmatrix} \frac{\boldsymbol{r}}{\lambda_1^3}\boldsymbol{t}_{11} & \frac{\boldsymbol{r}}{\lambda_2^3}\boldsymbol{t}_{12} & \frac{\boldsymbol{f}_{x1}}{\boldsymbol{r}\lambda_3^3}\boldsymbol{t}_{13} & \frac{\boldsymbol{f}_{x1}}{\boldsymbol{r}\lambda_4^3}\boldsymbol{t}_{14} \\ \frac{\boldsymbol{r}}{\lambda_1^2}\boldsymbol{t}_{21} & \frac{\boldsymbol{r}}{\lambda_2^2}\boldsymbol{t}_{22} & \frac{\boldsymbol{f}_{x1}}{\boldsymbol{r}\lambda_3^2}\boldsymbol{t}_{23} & \frac{\boldsymbol{f}_{x1}}{\boldsymbol{r}\lambda_4^2}\boldsymbol{t}_{24} \\ -\frac{1}{\lambda_1^2}\boldsymbol{t}_{31} & -\frac{1}{\lambda_2^2}\boldsymbol{t}_{32} & -\frac{1}{\lambda_3^2}\boldsymbol{t}_{33} & -\frac{1}{\lambda_4^2}\boldsymbol{t}_{34} \\ \frac{1}{\lambda_1}\boldsymbol{t}_{41} & \frac{1}{\lambda_2}\boldsymbol{t}_{42} & \frac{1}{\lambda_3}\boldsymbol{t}_{43} & \frac{1}{\lambda_4}\boldsymbol{t}_{44} \end{bmatrix}^{-1}$$

[†] The case when $\boldsymbol{f}_{x1}$ is zero is trivial and is solved separately; however, details are not presented here since the final results are found to be consistent with the general solution for non-zero $\boldsymbol{f}_{x1}$.

$$\boldsymbol{t}_{1i} = \boldsymbol{t}_{3i} \triangleq \left(1 + \lambda_1 - e^{\lambda_1}\right), \qquad \boldsymbol{t}_{2i} = \boldsymbol{t}_{3i} \triangleq \left(1 - e^{\lambda_1}\right)$$

We next make use of the natural boundary conditions at the free end of the beam. Natural boundary conditions involve relations between loads and displacements that occur naturally because of the beam governing equation. For the current case, these can be determined from the beam governing equations (18) applied at the free end of the beam i.e. at $x = 1$.

$$\begin{aligned} u_y''(1) &= -u_z'(1)\boldsymbol{m}_{x1} + \boldsymbol{m}_{z1} \\ u_y'''(1) &= -u_z''(1)\boldsymbol{m}_{x1} - \boldsymbol{f}_{y1} + \boldsymbol{f}_{x1}u_y'(1) \\ u_z''(1) &= u_y'(1)\boldsymbol{m}_{x1} - \boldsymbol{m}_{y1} \\ u_z'''(1) &= u_y''(1)\boldsymbol{m}_{x1} - \boldsymbol{f}_{z1} + \boldsymbol{f}_{x1}u_z'(1) \end{aligned} \quad (23)$$

The general solution for u_y and u_z are given by (21) is plugged into the above natural boundary conditions to relate the transverse loads $\boldsymbol{f}_{y1}$, $\boldsymbol{f}_{z1}$, $\boldsymbol{m}_{y1}$ and $\boldsymbol{m}_{z1}$ to the transverse displacements u_{y1}, u_{z1}, θ_{y1} and θ_{z1} by a stiffness matrix:

$$\begin{Bmatrix} \boldsymbol{f}_{y1} \\ \boldsymbol{m}_{z1} \\ \boldsymbol{f}_{z1} \\ \boldsymbol{m}_{y1} \end{Bmatrix} = [k] \begin{Bmatrix} u_{y1} \\ \theta_{z1} \\ u_{z1} \\ \theta_{y1} \end{Bmatrix}, \quad \text{where} \quad [k] \triangleq \{[A][B][C] + [D]\} \quad (24)$$

$$[A] \triangleq \begin{bmatrix} \boldsymbol{r} - \boldsymbol{m}_{x1} & \boldsymbol{r} - \boldsymbol{m}_{x1} & \frac{\boldsymbol{f}_{x1}}{\boldsymbol{r}} - \boldsymbol{m}_{x1} & \frac{\boldsymbol{f}_{x1}}{\boldsymbol{r}} - \boldsymbol{m}_{x1} \\ -\frac{\boldsymbol{r}}{\lambda} & \frac{\boldsymbol{r}}{\lambda} & -\frac{\lambda}{\boldsymbol{r}} & \frac{\lambda}{\boldsymbol{r}} \\ -\left(\lambda + \frac{\boldsymbol{r}\boldsymbol{m}_{x1}}{\lambda}\right) & \left(\lambda + \frac{\boldsymbol{r}\boldsymbol{m}_{x1}}{\lambda}\right) & -\left(\frac{\boldsymbol{f}_{x1}}{\lambda} + \frac{\lambda\boldsymbol{m}_{x1}}{\boldsymbol{r}}\right) & \left(\frac{\boldsymbol{f}_{x1}}{\lambda} + \frac{\lambda\boldsymbol{m}_{x1}}{\boldsymbol{r}}\right) \\ -1 & -1 & -1 & -1 \end{bmatrix}$$

$$[B] \triangleq \begin{bmatrix} e^{\lambda} & 0 & 0 & 0 \\ 0 & e^{\lambda} & 0 & 0 \\ 0 & 0 & e^{\frac{\boldsymbol{f}_{x1}}{\lambda}} & 0 \\ 0 & 0 & 0 & e^{-\frac{\boldsymbol{f}_{x1}}{\lambda}} \end{bmatrix}, \quad [D] \triangleq \begin{bmatrix} 0 & \boldsymbol{f}_{x1} & 0 & 0 \\ 0 & 0 & 0 & -\boldsymbol{m}_{x1} \\ 0 & 0 & 0 & -\boldsymbol{f}_{x1} \\ 0 & \boldsymbol{m}_{x1} & 0 & 0 \end{bmatrix}$$

The above relations show that the transverse end-loads and transverse end-displacements are linearly related by a stiffness matrix. This is expected because the bending direction beam governing equations (18) were also linear in these loads and displacements. However, the transverse stiffness matrix does include the axial force $\boldsymbol{f}_{x1}$ and twisting moment $\boldsymbol{m}_{x1}$. The individual stiffness terms, when stated in an explicit form, turn out to be very complicated transcendental expressions in $\boldsymbol{f}_{x1}$ and $\boldsymbol{m}_{x1}$, making it impossible to gauge the influence of these loads on the transverse stiffness. Therefore, to gain better insight, we carry out the Taylor series expansion of these transcendental expressions in terms of $\boldsymbol{f}_{x1}$ and $\boldsymbol{m}_{x1}$, as follows:

$$[k] = \begin{bmatrix} k_{11} & k_{12} & k_{15} & k_{16} \\ k_{21} & k_{22} & k_{25} & k_{26} \\ k_{51} & k_{52} & k_{55} & k_{56} \\ k_{61} & k_{62} & k_{65} & k_{66} \end{bmatrix} \quad (25)$$

$$k_{11} = k_{55} = \left(12 - \frac{1}{5}\boldsymbol{m}_{x1}{}^2 + \cdots\right) + \frac{6}{5}\boldsymbol{f}_{x1}\left(1 + \frac{2\boldsymbol{m}_{x1}{}^2}{315} + \cdots\right)$$
$$-\frac{1}{700}\boldsymbol{f}_{x1}{}^2\left(1 + \frac{31\boldsymbol{m}_{x1}{}^2}{34} + \cdots\right) + \cdots$$
$$k_{12} = k_{21} = -k_{56} = -k_{65} =$$
$$\left(-6 + \frac{1}{10}\boldsymbol{m}_{x1}{}^2 + \cdots\right) - \frac{1}{10}\boldsymbol{f}_{x1}\left(1 + \frac{4\boldsymbol{m}_{x1}{}^2}{105} + \cdots\right)$$
$$+\frac{1}{1400}\boldsymbol{f}_{x1}{}^2\left(1 + \frac{5\boldsymbol{m}_{x1}{}^2}{36} + \cdots\right) + \cdots$$
$$k_{22} = k_{66} = \left(4 - \frac{1}{20}\boldsymbol{m}_{x1}{}^2 + \cdots\right) + \frac{2}{15}\boldsymbol{f}_{x1}\left(1 + \frac{\boldsymbol{m}_{x1}{}^2}{70} + \cdots\right)$$
$$-\frac{11}{6300}\boldsymbol{f}_{x1}{}^2\left(1 + \frac{\boldsymbol{m}_{x1}{}^2}{44} + \cdots\right) + \cdots$$
$$k_{15} = k_{51} = 0, \quad k_{26} = -k_{62} = -\frac{1}{2}\boldsymbol{m}_{x1}$$
$$k_{16} = k_{61} = k_{25} = k_{52} = \boldsymbol{m}_{x1} - \frac{1}{60}\boldsymbol{f}_{x1}\boldsymbol{m}_{x1} + \cdots$$

In the stiffness matrix above, the subscripts 1 and 2 are related to the two end-displacements, u_{y1} and θ_{z1}, in the XY bending plane. Subscripts 5 and 6 are related to the two end-displacements, u_{z1} and θ_{y1}, in the XZ bending plane. Subscripts 3 and 4 are reserved for the X direction displacements, u_{x1} and θ_{x1}, respectively.

The above series expansions the transverse direction stiffness terms indeed shed more light on the effects of the axial load and twisting moment. First , it may be verified that in the absence of $\boldsymbol{f}_{x1}$ and $\boldsymbol{m}_{x1}$, the stiffness matrix coefficients relating u_{y1} and θ_{z1} to loads $\boldsymbol{f}_{z1}$ and $\boldsymbol{m}_{y1}$ and those relating u_{z1} and θy1 to loads $\boldsymbol{f}_{y1}$ and $\boldsymbol{m}_{z1}$ become zero, showing that the two bending directions are uncoupled, and the resulting stiffness matrix is same as one obtained from a purely linear analysis [6, 12]. Next we find that if $\boldsymbol{m}_{x1}$ is set to zero the two bending directions are still decoupled. Also, in each bending direction, the influence of the axial $\boldsymbol{f}_{x1}$ on transverse stiffness is identical to that seen in planar beams [5, 6], i.e. there is a prominent load-stiffening component associated with the first power of $\boldsymbol{f}_{x1}$.

Thus, it is clear that any coupling between the two bending directions arises solely from the twisting moment $\boldsymbol{m}_{x1}$. The displacement range of interest (u_y, u_z and $\theta_{Xd} \sim 0.1$) implies that the normalized twisting moment $\boldsymbol{m}_{x1}$ is also of the order of *0.1* (based on nominal linear twisting stiffness). In comparison, the normalized axial force $\boldsymbol{f}_{x1}$ can be of the order of *1* or greater since it is along a DoC (or load bearing) direction.

Given this magnitude of $\boldsymbol{m}_{x1}$, it may be seen that its contribution in the k_{11}, k_{12}, k_{22}, k_{55}, k_{56}, and k_{66} terms is less than *0.5%*, and therefore $\boldsymbol{m}_{x1}$ terms may be dropped altogether in these cases. Similarly, the second power and higher terms in $\boldsymbol{m}_{x1}$ may be dropped in k_{16} and k_{25} terms as well. However, the first power of $\boldsymbol{m}_{x1}$ that shows up only in the k_{26}, k_{62}, k_{25}, and k_{52} terms cannot be ignored, being the sole or most important contributor in each of these stiffness terms. In fact, it is these latter stiffness terms that give rise to cross-axis coupling between the two bending directions. Even though the coupling is weak, it captures a behavior that is not identified in a purely linear analysis.

Next, it may be seen that given the larger magnitude of $\boldsymbol{f}_{x1}$, its contribution to the transverse stiffness is stronger. In the stiffness terms k_{11}, k_{12}, k_{22}, k_{55}, k_{56}, and k_{66}, the first power in $\boldsymbol{f}_{x1}$ represents the load-stiffening effect, identical to that seen in planar beams [5, 6]. The second and higher power $\boldsymbol{f}_{x1}$ terms have a negligible contribution over the load and displacement range of interest, and can be dropped. However, as shown via energy arguments [16], the second power term should be retained to maintain consistency with the X direction constraint relation. Based on the above rationale for truncating higher order terms in the series expansions of expression (25), the final simplified form of transverse direction stiffness terms are summarized below:

$$\begin{aligned}
&k_{11} = k_{55} \approx 12 + \frac{6}{5}\boldsymbol{f}_{x1} - \frac{1}{700}\boldsymbol{f}_{x1}{}^2 \\
&k_{12} = k_{21} = -k_{56} = -k_{65} \approx -6 - \frac{1}{10}\boldsymbol{f}_{x1} + \frac{1}{1400}\boldsymbol{f}_{x1}{}^2 \\
&k_{22} = k_{66} \approx 4 + \frac{2}{15}\boldsymbol{f}_{x1} - \frac{11}{6300}\boldsymbol{f}_{x1}{}^2 \\
&k_{15} = k_{51} = 0, \quad k_{26} = -k_{62} = -\frac{1}{2}\boldsymbol{m}_{x1} \\
&k_{16} = k_{61} = k_{25} = k_{52} \approx \boldsymbol{m}_{x1} - \frac{1}{60}\boldsymbol{f}_{x1}\boldsymbol{m}_{x1}
\end{aligned} \tag{26}$$

This engineering approximation (truncation error) of the transcendental terms in the stiffness matrix produces less that *1%* error, while making the transverse direction load-displacement relation more insightful and simpler to work with for a designer.

Next, we proceed to determine the X direction load-displacement relation. The displacement in this direction can be split into two parts. The first part is a purely elastic component, which is given by the stretching of the beam arc-length due to $\boldsymbol{f}_{x1}$. The second part arises from the geometric constraint of beam-arc length conservation, and is captured by the integration below:

$$-\frac{1}{2}\int_0^1 \left(u_y'^2 + u_z'^2\right) dx \tag{27}$$

Using the solution of u_y and u_z given by Eq. (21), the above integral is carried out. The resulting expression comprises highly complicated transcendental functions of $\boldsymbol{f}_{x1}$ and $\boldsymbol{m}_{x1}$, which are not presented here for the sake of brevity. To allow greater design insight, these transcendental expressions are expanded in terms of $\boldsymbol{f}_{x1}$ and $\boldsymbol{m}_{x1}$. Using engineering approximations similar to above, the second and higher powers of $\boldsymbol{f}_{x1}$ and $\boldsymbol{m}_{x1}$ are truncated, while incurring an error of less than *1%* over the displacement and load ranges of interest. The resulting simplified expression for total axial displacement of the beam's end can be stated in the following compact form:

$$u_{x1} = \frac{\boldsymbol{f_{x1}}}{k_{33}} + \begin{Bmatrix} u_{y1} \\ \theta_{z1} \end{Bmatrix}^T \begin{bmatrix} -\frac{3}{5} & \frac{1}{20} \\ \frac{1}{20} & -\frac{1}{15} \end{bmatrix} \begin{Bmatrix} u_{y1} \\ \theta_{z1} \end{Bmatrix} + \begin{Bmatrix} u_{z1} \\ \theta_{y1} \end{Bmatrix}^T \begin{bmatrix} -\frac{3}{5} & -\frac{1}{20} \\ -\frac{1}{20} & -\frac{1}{15} \end{bmatrix} \begin{Bmatrix} u_{z1} \\ \theta_{y1} \end{Bmatrix}$$

$$+ \boldsymbol{f_{x1}} \begin{Bmatrix} u_{y1} \\ \theta_{z1} \end{Bmatrix}^T \begin{bmatrix} \frac{1}{700} & -\frac{1}{1400} \\ -\frac{1}{1400} & \frac{11}{6300} \end{bmatrix} \begin{Bmatrix} u_{y1} \\ \theta_{z1} \end{Bmatrix} + \boldsymbol{f_{x1}} \begin{Bmatrix} u_{z1} \\ \theta_{y1} \end{Bmatrix}^T \begin{bmatrix} \frac{1}{700} & \frac{1}{1400} \\ \frac{1}{1400} & \frac{11}{6300} \end{bmatrix} \begin{Bmatrix} u_{z1} \\ \theta_{y1} \end{Bmatrix}$$

$$= \frac{\boldsymbol{f_{x1}}}{k_{33}} + \begin{Bmatrix} u_{y1} \\ \theta_{z1} \\ u_{z1} \\ \theta_{y1} \end{Bmatrix}^T \begin{bmatrix} g_{11} & g_{12} & g_{15} & g_{16} \\ g_{21} & g_{22} & g_{25} & g_{26} \\ g_{51} & g_{52} & g_{55} & g_{56} \\ g_{61} & g_{62} & g_{65} & g_{66} \end{bmatrix} \begin{Bmatrix} u_{y1} \\ \theta_{z1} \\ u_{z1} \\ \theta_{y1} \end{Bmatrix} \quad , \quad \text{where} \tag{28}$$

$$g_{11} = g_{55} \approx -\frac{3}{5} + \boldsymbol{f_{x1}} \frac{1}{700}, \qquad g_{22} = g_{66} \approx -\frac{1}{15} + \boldsymbol{f_{x1}} \frac{11}{6300}$$

$$g_{12} = g_{21} = -g_{56} = -g_{65} \approx \frac{1}{20} - \boldsymbol{f_{x1}} \frac{1}{1400},$$

$$g_{15} = g_{16} = g_{26} = g_{26} = g_{51} = g_{52} = g_{61} = g_{62} \approx 0$$

$$k_{33} \triangleq \frac{12L^2}{T_Y^{\,2}}$$

The first term in Eq.(28) is a purely elastic term, independent of any other displacements. This term represents the elastic stretching of the beam's arc-length, with k_{33} being the normalized elastic stiffness. The subsequent matrix in this equation is the consequence of beam arc-length conservation condition. The first term in the series expansion of the g terms is independent of the loads $\boldsymbol{f_{x1}}$ and $\boldsymbol{m_{x1}}$. This implies that a certain component of the axial displacement is solely dependent on the transverse direction DoF displacements, and therefore represents a purely kinematic component. Next, the first power of $\boldsymbol{f_{x1}}$ shows in some of the series expansions. This term depends both on the X DoC load as well as the transverse DoF displacement, and is therefore referred to as the elastokinematic term. It is important to include this term in the final simplified expressions of g, because it is comparable to the purely elastic term for the transverse DoF displacement range of interest. Higher power $\boldsymbol{f_{x1}}$ terms may be dropped given their insignificant contribution.

It is interesting to note that in the series expansion of the g terms, no linear dependence on the twisting moment $\boldsymbol{m_{x1}}$ is found. The second and higher powers of $\boldsymbol{m_{x1}}$ that do show up have a negligible impact on the total X displacement, and are, therefore, dropped at the truncation step.

Ultimately, it may be seen that the kinematic and elastokinematic terms that are retained in final form of the axial displacement, are simply the sum of the respective kinematic and elastokinematic terms arising from each bending direction (Y and Z). The kinematic component generally dominates the axial displacement in terms of magnitude, and dictates the parasitic error motion in this DoC direction. But being purely kinematic in nature, it does not contribute to the stiffness in this DoC direction. On the other hand, the elastokinematic component, while small in magnitude, makes an important contribution to the axial compliance, and therefore plays an important role in DoC characterization.

Finally, we move on to the twisting of the beam. As a first step, the relation between θ_X and θ_{Xd} can be determined to be as follows [17]:

$$\theta_{x1} \approx \theta_{xd1} - \frac{1}{2} u'_{y1} u'_{z1} = \theta_{xd1} + \frac{1}{2} \theta_{y1} \theta_{z1} \tag{29}$$

The first order differential equation of the twist angle θ_{xd} in the deformed co-ordinate axis $X_d Y_d Z_d$ is given in Eq.(13)(i). Using the normalization scheme presented earlier, substituting the solutions for u_y and u_z from Eq.(21), and employing the relation of Eq.(29), the twist angle at the end of the beam, θ_{x1}, may be determined in terms of end-loads and remaining end-displacements. As expected, the result comprises transcendental functions of $\boldsymbol{f_{x1}}$ and $\boldsymbol{m_{x1}}$. To allow greater design insight and mathematical simplicity, these transcendental expressions are expanded in terms of $\boldsymbol{f_{x1}}$ and $\boldsymbol{m_{x1}}$. Using engineering approximations justified over the load and displacement ranges of interest, only the first powers of $\boldsymbol{f_{x1}}$ and $\boldsymbol{m_{x1}}$ are found to be relevant; the rest are truncated, while incurring an error of less than *1%*. The resulting simplified expression for beam end twist angle can be stated in the following compact form:

$$\theta_{x1} \approx \frac{\boldsymbol{m_{x1}}}{k_{44}} + \begin{Bmatrix} u_{y1} \\ \theta_{z1} \\ u_{z1} \\ \theta_{y1} \end{Bmatrix}^T \begin{bmatrix} e_{11} & e_{12} & e_{15} & e_{16} \\ e_{21} & e_{22} & e_{25} & e_{26} \\ e_{51} & e_{52} & e_{55} & e_{56} \\ e_{61} & e_{62} & e_{65} & e_{66} \end{bmatrix} \begin{Bmatrix} u_{y1} \\ \theta_{z1} \\ u_{z1} \\ \theta_{y1} \end{Bmatrix} =$$

$$\frac{\boldsymbol{m_{x1}}}{k_{44}} + \begin{Bmatrix} u_{y1} \\ \theta_{z1} \\ u_{z1} \\ \theta_{y1} \end{Bmatrix}^T \begin{bmatrix} 0 & 0 & 0 & c_1 \\ 0 & 0 & c_1 & 0 \\ 0 & c_1 & 0 & 0 \\ c_1 & 0 & 0 & 0 \end{bmatrix} \begin{Bmatrix} u_{y1} \\ \theta_{z1} \\ u_{z1} \\ \theta_{y1} \end{Bmatrix} + \boldsymbol{m_{x1}} \begin{Bmatrix} u_{y1} \\ \theta_{z1} \\ u_{z1} \\ \theta_{y1} \end{Bmatrix}^T \begin{bmatrix} c_2 & c_3 & 0 & 0 \\ c_3 & c_4 & 0 & 0 \\ 0 & 0 & c_2 & c_3 \\ 0 & 0 & c_3 & c_4 \end{bmatrix} \begin{Bmatrix} u_{y1} \\ \theta_{z1} \\ u_{z1} \\ \theta_{y1} \end{Bmatrix}$$

$$+ \boldsymbol{f_{x1}} \begin{Bmatrix} u_{y1} \\ \theta_{z1} \\ u_{z1} \\ \theta_{y1} \end{Bmatrix}^T \begin{bmatrix} 0 & 0 & 0 & c_5 \\ 0 & 0 & c_5 & 0 \\ 0 & c_5 & 0 & 0 \\ c_5 & 0 & 0 & 0 \end{bmatrix} \begin{Bmatrix} u_{y1} \\ \theta_{z1} \\ u_{z1} \\ \theta_{y1} \end{Bmatrix} \tag{30}$$

where $k_{44} \triangleq \dfrac{1}{1+\nu}$, $c_1 \triangleq -\dfrac{1}{2} + \dfrac{3}{k_{44}}$, $c_2 \triangleq \dfrac{1}{5} + \dfrac{3}{5k_{44}}$

$c_3 \triangleq -\dfrac{1}{10} - \dfrac{1}{20k_{44}}$, $c_4 \triangleq \dfrac{1}{20} + \dfrac{1}{15k_{44}}$, $c_5 \triangleq \dfrac{1}{120} + \dfrac{1}{20k_{44}}$

Foremost, it is important to note that unlike the transverse DoF directions, where loads were expressed in terms of stiffness and displacements, it is mathematically more convenient to express the twisting DoF rotation in terms of the twisting moment and the transverse DoF displacements. This is somewhat similar in format to the axial DoC displacement expression (28).

The first term in Eq.(30) is independent of any other displacements and arises simply from the elastic twisting of the beam. It is therefore the purely elastic component of θ_{x1}. The second term in Eq. (30), is free of any loads, and entirely dependent on the transverse DoF displacements, thus representing a purely kinematic component of the twist angle, similar to the kinematic component seen in the axial DoC displacement. However, unlike that case, the magnitude of the kinematic component here is relatively smaller than the purely elastic component for nominal twisting moment and transverse displacements; it becomes the most important contributor in the absence of a twisting moment. The third term in Eq. (30) has a dependence on the twisting moment $\boldsymbol{m}_{x1}$ as well as the transverse DoF displacements. This is also similar to the elastokinematic component seen in the axial DoC displacement. An important difference in this case is that, since $1/k_{44}$ is of order 1 and the elastokinematic coefficients are each multiplied by two DoF displacements, each of order 0.1, the net contribution of the whole elastokinematic term to the overall θ_{x1} and stiffness in the twisting direction is less than 1% of their actual values. Hence the elastokinematic term for θ_{x1} is dropped this point onwards. The last term above represents a component that depends on the axial DoC load $\boldsymbol{f}_{x1}$ and the transverse DoF displacements – a new kind of elastokinematic term not see earlier – because load dependence is not on $\boldsymbol{m}_{x1}$ but instead on $\boldsymbol{f}_{x1}$. This is a new kind of effect that is not ignorable. Overall, the twisting direction DoF exhibits a peculiar constraint behavior by borrowing certain attributes that have been associated with the DoC directions in the past [5, 6, 16].

5. MODEL VALIDATION VIA FINITE ELEMENT ANALYSIS (FEA)

The load displacement relationship, given by Eq.(25), shows that in the absence of twisting moment $\boldsymbol{m}_{x1}$, the displacements in the two bending plane XY and XZ are decoupled. In this case, the beam bends in each plane exactly like a planar beam whose stiffness coefficients k_{11}, k_{12}, k_{21}, k_{22}, k_{55}, k_{56}, k_{65} and k_{66} have been verified in our previous research [5, 6]. The remaining stiffness terms being non-zero in the presence of $\boldsymbol{m}_{x1}$ give rise to new coupling terms. Owing to the partial symmetry of the stiffness matrix $[k]$ $\left(\text{i.e. } k_{ij}=k_{ji},\ \ \forall\ \ (i,j)-\{(2,6),(6,2)\}\right)$, verifying only k_{15}, k_{16}, k_{26}, k_{62} should fully verify the stiffness terms associated with this coupling. New notation is introduced at this point to identify the coefficients within a stiffness term k_{ij} with the powers of $\boldsymbol{f}_{x1}$ and $\boldsymbol{m}_{x1}$ that it shows up with. These coefficient have two superscripts in parenthesis – the first signifying the power of $\boldsymbol{f}_{x1}$ and the second signifying the power of $\boldsymbol{m}_{x1}$. For example, the coefficient of the load-free term in k_{11} is denoted by $k_{11}^{(0)-(0)}$, signifying zero powers of $\boldsymbol{f}_{x1}$ and $\boldsymbol{m}_{x1}$. This notation is also used to represent the coefficients of different powers of $\boldsymbol{f}_{x1}$ and $\boldsymbol{m}_{x1}$ for e_{ij} and g_{ij}.

For the FEA simulations, the beam dimensions were taken to be: $L = 0.5$m, $T_Y=T_Z=0.02$m and the elastic modulus E and Poisson ratio ν was taken as 210 GPa and 0.3 respectively. Fig.4 plots the coefficient of $\boldsymbol{m}_{x1}$ for the total range of normalized transverse DoF displacements from -0.1 to 0.1 in the stiffness terms k_{15}, k_{16}, k_{26}, k_{62}. The FEA points are plotted in blue circles and crosses while the theoretical coefficients are shown by black line. Based on these results, the theoretical stiffness coefficients are found to be within 1% of the corresponding FEA values for two values of twisting moment $\boldsymbol{M}_{XL}$ at 200Nm and 400 Nm, corresponding to normalized values of 0.0357 and 0.0714, respectively.

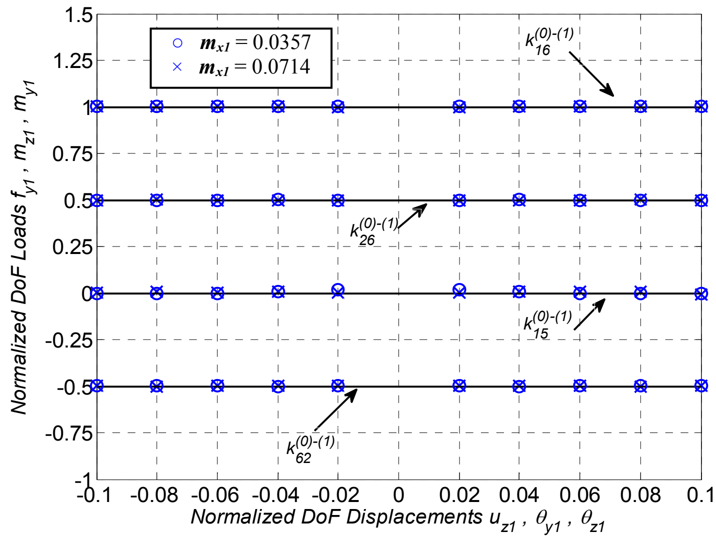

Fig.4: Cross-axis coupling stiffness coefficients

The geometric constraint term (the 'g' matrix in Eq.(28)) associated with the axial DoC are verified against FEA next. The kinematic and elastokinematic components of the axial displacement in Eq.(28) represent a sum of the individual kinematic and elastokinematic components arising from the two bending planes. The analytical results predict no significant effect of the twisting moment $\boldsymbol{m}_{x1}$ in this direction. This is corroborated by the FEA but not show here because the results are exactly the same as those reported for planar beams previously [5].

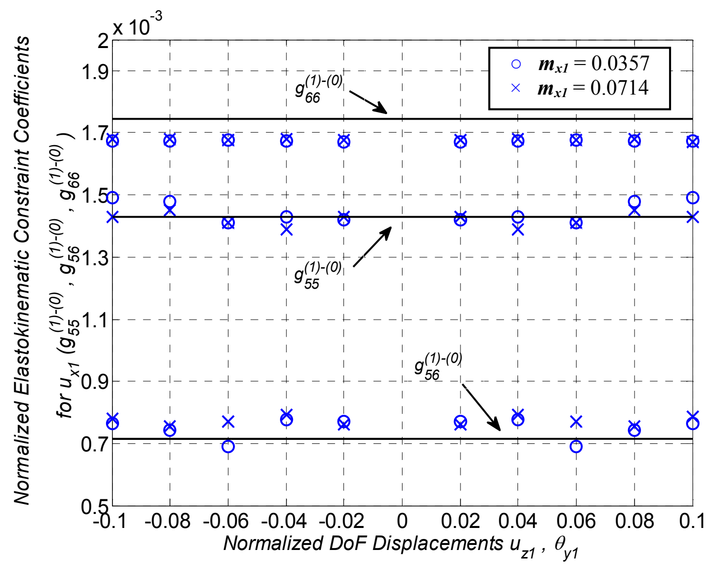

Fig. 5: Elastokinematic coefficients in DoC x-Displacement

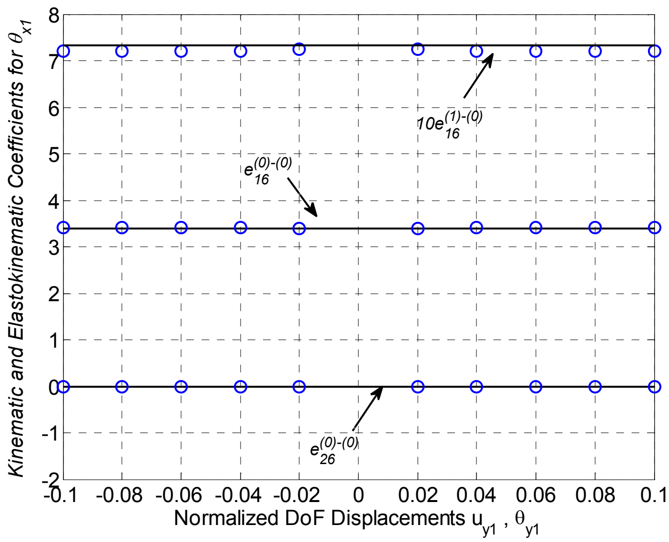

Fig. 6: Kinematic and elastokinematic coefficients in θ_{x1} displacement

The elastokinematic terms, a property of beam shape, is given in terms the elastokinematic coefficients $g_{11}^{(1)-(0)}$, $g_{12}^{(1)-(0)}$, $g_{21}^{(1)-(0)}$, $g_{22}^{(1)-(0)}$, $g_{55}^{(1)-(0)}$, $g_{56}^{(1)-(0)}$, $g_{65}^{(1)-(0)}$ and $g_{66}^{(1)-(0)}$. Using the symmetry of the 'g' matrix it is sufficient to verify only three coefficients $g_{55}^{(1)-(0)}$, $g_{56}^{(1)-(0)}$ and $g_{66}^{(1)-(0)}$. Figure 5 verifies these coefficients for two values of $\boldsymbol{m_{x1}}$. The errors, encountered comparing these geometric coefficients for spatial beam, are similar to that for planar beam implying negligible effect of $\boldsymbol{m_{x1}}$. The theoretical geometric coefficients were found to be with *3%* error of those predicted by FEA.

The FEA validation of the twisting DoF rotation, θ_{x1}, is given in Fig.6. To verify the kinematic matrix in Eq.(30), we set $\boldsymbol{m_{x1}}$ and $\boldsymbol{f_{x1}}$ to zero. One of the non-zero coefficients $e_{16}^{(0)-(0)}$ is verified in Fig.6. This matrix also shows a interesting property that a combination of similar displacements (both translational or both rotational) in the two bending plane does not produces any kinematic axial rotation. This is verified by $e_{25}^{(0)-(0)}$ in Fig.6.

Next we verify elastokinematic matrix with respect to $\boldsymbol{f_{x1}}$ of the twisting angle in Eq. (30). For this FEA simulation, $\boldsymbol{f_{x1}}$ is set to one and $e_{16}^{(1)-(0)}$, which is analytically predicted to be $\left(\frac{1}{120}+\frac{1+\nu}{20}\right)$, is verified.

5. CONCLUSION AND SUMMARY

In this paper, we have presented a compact, parametric, and closed-form model for the load-displacement relations of a uniform-thickness symmetric cross-section spatial beam, to help characterize its constraint behavior. The latter is strongly influenced by non-linear effects (loading-stiffening, kinematic, and elastokinematic) that are not captured in a purely linear elastic formulation. On the other hand, FEA, which captures all sources of non-linearities, does not offer much physical or analytical insight towards constraint-based flexure mechanism design.

Therefore, in developing a new model for the spatial beam, we choose to retain non-linearities associated with geometric arc-length conservation and application of load equilibrium in deformed configuration, which are relevant to the beam's constraint behavior and are not ignorable in the load and displacement range of interest. However, the non-linearity associated with beam curvature is dropped because it does not have any serious implications in terms of constraint behavior, and yet makes a closed-form analysis impossible. Furthermore, in the process of deriving a final set of end-load / end-displacement relations for the spatial beam while incorporating the above relevant non-linearities, several engineering approximations are made and appropriately justified, so that the resulting model is compact, parametric, and closed-form. The final result, which may be referred to as the spatial Beam Constraint Model, offers several insights into the DoF (Y, Z, Θ_Y, Θ_Z, and Θ_X) and DoC (X) behavior of the beam flexure.

It becomes clear that the four transverse bending DoF exhibit load-stiffening in the presence of axial DoC load $\boldsymbol{f_{x1}}$. This is expected based on planar beam results. However, an additional phenomenon noticed in the spatial beam is that the twisting DoF moment $\boldsymbol{m_{x1}}$ tends to provide coupling between the two beam bending directions. In the absence of this moment, the spatial beam behaves like two independent and orthogonal planar beams. However, in the presence of this twisting moment, bending force and moment from one bending plane results in a bending displacement and rotation in the other bending plane.

The spatial BCM also shows that there are no new effects seen in the X DoC direction. In addition to a purely elastic component in this axial direction, the kinematic and elastokinematic components are simply the sum of individual kinematic and elastokinematic components arising from the two bending planes. The presence of a twisting angle or moment plays no noticeable role here.

Finally, the most important new observation made via this model is with respect to the axial twisting DoF. In addition to a purely elastic dependence on the twisting moment $\boldsymbol{m_{x1}}$, θ_{x1} also comprises a purely kinematic component dependent on the transverse DoF displacements, as well as an elastokinematic term dependent on $\boldsymbol{f_{x1}}$ and the transverse DoF displacements. This is unique for a DoF, because kinematic and elastokinematic effects have generally been associated with DoC displacements in the past.

We envision that the above qualitative and quantitative understanding of the constraint characteristics of the spatial beam will facilitate the constraint-based design and optimization of 3D flexure mechanisms that employ such beam flexures. To further improve the utility of the proposed model, we plan to generalize it to incorporate variable cross-section, non-symmetric beams with initial curvature. Also a strain energy formulation, consistent with the proposed model, is being developed to facilitate the closed-form analysis of more complex 3D flexure mechanism geometries.

This research was supported in part by a National Science Foundation grant (CMMI # 0846738).

REFERENCES

1. Jones, R.V., 1988, *Instruments and Experiences: Papers on Measurement and Instrument Design*, John Wiley & Sons, New York, NY
2. Slocum, A.H., 1992, *Precision Machine Design*, Society of Manufacturing Engineers, Dearborn, MI.
3. Smith, S.T., 2000, *Flexures: Elements of Elastic Mechanisms*, Gordon and Breach Science Publishers, New York, NY
4. Blanding, D.K., 1999, *Exact Constraint: Machine Design Using Kinematic Principles*, ASME Press, New York, NY
5. Awtar, S., Slocum, A.H., and Sevincer, E., 2006, "Characteristics of Beam-based Flexure Modules", ASME Journal of Mechanical Design, 129 (6), pp 625-639
6. Awtar, S., and Sen, S., 2009, "A Generalized Constraint Model for Two-dimensional Beam Flexures", Proc. ASME IDETC/CIE 2009, San Diego CA, Paper # 87808
7. Hodges, D.H., 1984, "Proper Definition of Curvature in Nonlinear Beam Kinematics", AIAA Journal, **22**(12), pp 1825-1827
8. Hodges, D. H. and Dowell, E. H., 1974, "Nonlinear equations of motion for the elastic bending and torsion of twisted nonuniform rotor blades," *NASA Technical Note D-7818*
9. Mayo, J., and Dominguez, J., 1992, "Geometrically Nonlinear Coupling between Axial and Flexural Modes of Deformation of Multibody Systems", *Dynamics of Flexible Multibody Systems: Theory and Experiments*, Winter Annual Meeting of ASME, Anaheim CA, AMD-v.**141**, DSC-v.**37**, pp 95-103
10. Avramov, K.V. , Pierre, C. and Shyriaieva, N., 2007, "Flexural-flexural-torsional Nonlinear Vibrations of Pre-twisted Rotating Beams with Asymmetric Cross-sections", Journal of Vibration and Control, **13**(4), pp329-364
11. Dokumaci, E., 1987, "An Exact Solution for Coupled Bending and Torsion Vibrations of Uniform Beams Having Single Cross-sectional Symmetry", Journal of Sound and Vibration, **131** (3), pp 443-449
12. Crandall, S. H., Dahl, N. C., and Lardner T. J., 1972, *An Introduction to the Mechanics of Solids*, McGraw-Hill Book Company, NY
13. Baruh, H., 1999, *Analytical Dynamics*, McGraw-Hill, NY
14. Novozhilov, V. V., 1953, *Foundations of the Nonlinear Theory of* Elasticity, Graylock Press, Rochester, NY
15. Chen, C., 1999, *Linear Sytem Theory and Design,* Oxford University Press, NY
16. Awtar, S., and Sen, S., 2010, "Beam Constraint Model: A Non-Linear Strain Energy Formulation for Generalized Two-Dimensional Beam Flexures", Proc. ASME IDETC/CIE 2010, Montreal, Canada, Paper # 28184
17. Przemieniecki, J. S., 1968, *Theory of Matrix Structural Analysis*, McGraw-Hill, New York